New criterion for the existence of dark matter in neutron stars

Hongyi Sun and Dehua Wen*

School of Physics and Optoelectronics, South China University of Technology, Guangzhou 510641, People's Republic of China

(Received 10 October 2023; revised 11 April 2024; accepted 3 June 2024; published 24 June 2024)

The tidal deformability and the radius of neutron stars are observables, which have been used to constrain the neutron star equation of state and explore the composition in neutron stars. We investigated the radius and tidal deformability of dark matter admixed neutron stars (DANSs) by utilizing the two-fluid TOV (Tolman-Oppenheimer-Volkoff) equation. Assuming that the dark matter modeled as fermions (with or without self-interaction) or self-interacting bosons, for a series of DANSs at a fixed mass, it is shown that there exists the DANSs with smaller normal matter radii but larger tidal deformabilities. This negative correlation does not exist in the normal neutron stars. In other words, if the observation finds that the neutron stars with a fixed mass exists such a situation, that is, having a smaller observed radius but a larger tidal deformability, it will indicate the existence of dark matter in neutron stars. In addition, the relevant neutron star observations can also be used to constrain the dark matter parameters.

DOI: 10.1103/PhysRevD.109.123037

I. INTRODUCTION

Despite years of research and efforts, the essence of dark matter remains a mystery. There are several prospective particle candidates for the dark matter (such as weakly interacting massive particles (WIMPs), light bosons, and sterile neutrinos [1,2]). The interaction between the dark matter and the normal matter is mainly gravity, so a neutron star (one of the most compact objects in the universe) can capture a sizable amount of dark matter through its strong gravitational field. The accretion of dark matter into a neutron star can affect its macroscopic properties [3,4], which can be used to extract information about the dark matter. In all, neutron stars provide a new way to investigate the nature of dark matter.

Recently, the mass-radius measurements from the Neutron Star Interior Composition Explorer (NICER) [5–8] have yielded important constraints about the equations of state (EOSs) of dense nuclear matter [9,10]. Besides, the observation of the binary neutron star merger, the GW170817 event [11], has constrained the tidal deformability of a $M = 1.4M_\odot$ neutron star to a relatively small value ($\Lambda_{1.4} = 190^{+390}_{-120}$ [12]), which favors a soft EOS. Numerous of investigations have used these observations to obtain constraints on the properties of neutron stars and the parameters of EOS, such as the moment of inertia of neutron star [13–16], the sound speed [17–19] and the symmetry energy [20–22] of nuclear matter.

Theoretically, the capture of dark matter will further influence the mass, radius and tidal deformability of neutron stars [23–26], and even lead to the appearance of supermassive neutron stars [27]. The gravitational wave signal and the dynamics of the binary neutron star merger are also affected by the existence of dark matter [28–31]. The constraints on dark matter parameters obtained from the existing and future neutron star observations have also received extensive attentions [32–34]. In addition, the understanding of the interaction between the dark matter and the normal matter is still ambiguous. Except for the gravitational interaction, other interactions between the dark matter and the normal matter will soften the EOS, reducing the maximum mass of neutron stars [35] and the tidal deformability [36].

Furthermore, the accumulation of dark matter in a neutron star will lead to the emergence of a new type of compact star, i.e., dark matter admixed neutron stars (DANSs) [37–41]. Similar to the normal neutron stars, if the gravitational interaction between the dark matter and the normal matter is only considered, it is found that the maximum mass of DANS corresponds to the beginning of the unstable sequence [42]. For different types of dark matter candidates, such as fermionic dark matter [38,39], self interacting bosonic dark matter [40,41], and mirror dark matter [4,43], by adjusting the particle mass of dark matter and the interaction between the dark matter particles, DANSs with mass similar to the normal neutron stars can be obtained [44,45]. In addition, if the dark matter mass fraction (i.e. the mass proportion of dark matter in DANSs) is large or the particle mass of dark matter is small, the dark matter radius tends to be greater than that of normal matter, forming a dark matter halo around the DANS [32]. Conversely, a small dark matter mass fraction and a large

*Contact author: wendehua@scut.edu.cn

particle mass will lead to the occurrence of a dark matter core [38]. Based on different processes of the DANS formation [39], (for example, the remnant of the merger of a pure dark matter star [46,47] and a neutron star may be a DANS with a large dark matter mass fraction [4]), DANSs with different dark matter mass fractions can be formed.

In this work, the self-interacting bosons [48], the ideal Fermi gas [44,49] and the self-interacting fermions [50,51] are used to model the dark matter. Although other dark matter candidates, such as axions [27,52], self-interacting fermions [23,38], and the mirror twin Higgs model [53], may be more realistic, the two selected dark matter models are sufficient for a quantitative investigation of the concerned properties of DANSs. Moreover, we only consider the gravitational interaction between the dark matter and the normal matter, so the two-fluid TOV equations [43] are utilized to describe the DANSs. The influence of the dark matter on the structure and the properties of DANSs is investigated under different dark matter parameters. In addition, we focus on the change of the tidal deformability and the normal matter radius of DANSs, aiming to identify a way to prove the existence of dark matter in neutron stars by utilizing the uniqueness of DANS observables.

This paper is organized as follows. In Sec. II, the basic formulas for the macroscopic properties of DANSs are briefly introduced. In Sec. III, the normal matter radius and the tidal deformability of DANSs with different dark matter parameters and different normal matter EOSs are presented. Finally, a summary is given in Sec. IV.

II. BASIC FORMULAS FOR THE MACROSCOPIC PROPERTIES OF DANS

A. Two-fluid TOV equations

In contrast to a nonrotating neutron stars with only one component, the individual components of a static neutron star with two fluids that only interact through gravity need to be calculated independently, i.e., using the two-fluid TOV equations [41,43]

$$\frac{dp_i}{dr} = -\frac{G\varepsilon_i(r)M(r)}{c^2r^2}\left(1+\frac{p_i(r)}{\varepsilon_i(r)}\right) \times \left(1+\frac{4\pi r^3 p(r)}{M(r)c^2}\right)\left(1-\frac{2GM(r)}{c^2 r}\right)^{-1}, \quad (1)$$

$$\frac{dM_i}{dr} = \frac{4\pi r^2 \varepsilon_i(r)}{c^2}, \quad (2)$$

where i represents the two different components ($i = N$ or D denotes the normal matter or the dark matter). $p_i(r)$, $\varepsilon_i(r)$, and $M_i(r)$ are the pressure, energy density, and mass of the two components at radius r, respectively. Variables without a subscript denote the sums of the two components [i.e., $M(r) = M_N(r) + M_D(r)$, $p(r) = p_N(r) + p_D(r)$]. The initial condition at the center of a neutron star are $M_i(0) = 0$ and $p_i(0) = p_{c,i}$. The pressures of the two components will drop to 0 at different radii, then the mass and the radius of each component can be obtained. Due to the fact that the dark matter is electromagnetically dark, we focus on investigating the normal matter radius (R_N).

B. Tidal deformability

The tidal deformability of a normal neutron star characterizes the deformation of the neutron star due to the tidal effect created by a companion star. The details of the computation of the tidal deformability for nonrotating neutron stars can be found in Refs. [54]. Here we only introduce the main equations. The tidal deformability is defined as

$$\lambda = \frac{2}{3}R^5 k_2. \quad (3)$$

The second (quadrupole) tidal Love number k_2 can be obtained from [54,55]

$$\begin{aligned} k_2 = {} & \frac{8}{5}x^5(1-2x)^2(2-y_R+2x(y_R-1)) \\ & \times (2x(6-3y_R+3x(5y_R-8)) \\ & + 4x^3(13-11y_R+x(3y_R-2)+2x^2(1+y_R)) \\ & + 3(1-2x)^2(2-y_R+2x(y_R-1))\ln(1-2x))^{-1}, \end{aligned} \quad (4)$$

where $x = GM/Rc^2$ is the compactness of neutron stars, and y_R is determined by

$$r\frac{dy(r)}{dr} + y(r)^2 + y(r)F(r) + r^2Q(r) = 0, \quad (5)$$

with $F(r)$ and $Q(r)$ are functions of $M(r)$, $p(r)$ and $\varepsilon(r)$ [55]

$$F(r) = \left[1-\frac{4\pi r^2 G}{c^4}(\varepsilon(r)-p(r))\right]\left(1-\frac{2M(r)G}{rc^2}\right)^{-1}, \quad (6)$$

$$\begin{aligned} r^2Q(r) = {} & \frac{4\pi r^2 G}{c^4}\left[5\varepsilon(r)+9p(r)+\frac{\varepsilon(r)+p(r)}{\partial p(r)/\partial\varepsilon(r)}\right] \\ & \times \left(1-\frac{2M(r)G}{rc^2}\right)^{-1} - 6\left(1-\frac{2M(r)G}{rc^2}\right)^{-1} \\ & - \frac{4M^2(r)G^2}{r^2c^4}\left(1+\frac{4\pi r^3 p(r)}{M(r)c^2}\right)^2\left(1-\frac{2M(r)G}{rc^2}\right)^{-2}, \end{aligned} \quad (7)$$

then $y(r) = y_R$ at the radius R of the neutron star is provided, and the dimensionless tidal deformability is given by

$$\Lambda = \lambda\left(\frac{GM}{c^2}\right)^{-5} = \frac{2}{3}k_2\left(\frac{Rc^2}{GM}\right)^5. \tag{8}$$

For a DANS with two fluids, Eq. (7) should be modified. Specifically, the term with $\partial p(r)/\partial\varepsilon(r)$ should be changed to

$$\frac{\varepsilon + p}{\partial p/\partial\varepsilon} \to \sum_i \frac{\varepsilon_i + p_i}{\partial p_i/\partial\varepsilon_i}, \tag{9}$$

and the energy density, pressure, and mass in Eqs. (6) and (7) should be replaced by the two components' sums. Additionally, the total radius R in Eq. (8) is the larger one of the normal matter radius R_N and the dark matter radius R_D.

C. Dark matter modeled as self-interacting bosons

Due to the absence of the degeneracy pressure in bosonic matter, it is necessary to assume the presence of self-interaction in bosonic dark matter to resist gravity. The EOS for the self-interacting bosonic dark matter [32,48] can be written as

$$p = \frac{4\rho_0 c^2}{9}\left(\sqrt{1 + \frac{3\rho}{4\rho_0}} - 1\right)^2 \tag{10}$$

in the strong-coupling limit [48], where $\rho_0 = m_{\chi,b}^4/4\lambda\hbar^3c^5$, and $m_{\chi,b}$, ρ, and λ are the particle mass, density, and coupling constant of the self-interacting bosonic dark matter. From Eq. (10), it is evident that increasing $m_{\chi,b}$ and decreasing λ have similar effects on the EOS of bosonic dark matter, as the effective parameter is $m_{\chi,b}^4/\lambda$. In the following, the coupling constant is fixed to $\lambda = \pi$ (which satisfies the strong-coupling limit) and we only consider the impact of $m_{\chi,b}$ on DANSs.

D. Dark matter modeled as ideal Fermi gas

Moreover, we assume the dark matter to be made of ideal Fermi gas and neglect finite temperature effects. Although this model is considered relatively simplistic, it still provides us with quantitative insights into the properties of DANS [44]. Assuming there is only one type of dark matter particle with spin $\frac{1}{2}$, the ideal Fermi gas EOS [44,49] at zero temperature is

$$\varepsilon = K(\sinh t - t), \tag{11}$$

$$p = \frac{K}{3}\left(\sinh t - 8\sinh\frac{t}{2} + 3t\right), \tag{12}$$

with

$$K = \frac{\pi m_{\chi,f}^4}{32\pi^3(\hbar c)^3}, \tag{13}$$

$$t = 4\ln(y + \sqrt{1 + y^2}), \tag{14}$$

where y is a variable related to the number density n

$$y = \left(\frac{3\pi^2(\hbar c)^3 n}{m_{\chi,f}^3}\right)^{1/3}, \tag{15}$$

and $m_{\chi,f}$ is the particle mass, which is also the only adjustable parameter of the ideal Fermi gas EOS.

E. Dark matter modeled as self-interacting fermions

In order to investigate the effects of self-interaction on the fermionic dark matter, the exchange of scalar and vector mesons is used to describe the interaction of the fermionic dark matter. The Lagrangian density for the self-interacting fermionic dark matter with meson exchange can be written as [50,51]:

$$\begin{aligned}\mathcal{L}_D = {}& \bar{\psi}_D[\gamma_\mu(i\partial^\mu - g_V V^\mu) - (m_{\chi,f} - g_\phi\phi)]\psi_D \\ & + \frac{1}{2}(\partial_\mu\phi\partial^\mu\phi - m_\phi^2\phi^2) + \frac{1}{2}m_V^2 V_\mu V^\mu \\ & - \frac{1}{4}(\partial_\mu V_\nu - \partial_\nu V_\mu)(\partial^\mu V^\nu - \partial^\nu V^\mu),\end{aligned} \tag{16}$$

where $m_{\chi,f}$ is the mass of dark matter in vacuum, and g_i (m_i) are the coupling constant (meson mass) of dark matter ($i = V, \phi$). The energy density ε_D and pressure p_D of dark matter are given in the following form:

$$\begin{aligned}\varepsilon_D = {}& \frac{2}{(2\pi)^3}\int_0^{k_{F,D}} d^3k\sqrt{k^2 + m_{\chi,f}^{*2}} + \frac{g_V^2}{2m_V^2}\rho_D^2 \\ & + \frac{m_\phi^2}{2g_\phi^2}(m_{\chi,f} - m_{\chi,f}^*)^2,\end{aligned} \tag{17}$$

$$\begin{aligned}p_D = {}& \frac{2}{3(2\pi)^3}\int_0^{k_{F,D}} d^3k\frac{k^2}{\sqrt{k^2 + m_{\chi,f}^{*2}}} + \frac{g_V^2}{2m_V^2}\rho_D^2 \\ & - \frac{m_\phi^2}{2g_\phi^2}(m_{\chi,f} - m_{\chi,f}^*)^2,\end{aligned} \tag{18}$$

where $m_{\chi,f}^* = m_{\chi,f} - g_\phi\phi_0$ is the effective mass of dark matter, and $\rho_D = \frac{k_{F,D}^3}{3\pi^2}$ is the dark matter density. Furthermore, the repulsive (attractive) interaction, which will stiffen (soften) the dark matter EOS, is just determined by the ratio parameter $C_{DV} = g_V/m_V$ ($C_{DS} = g_\phi/m_\phi$). So we adopt $C_{DV} = 10\ \mathrm{GeV}^{-1}$ and $C_{DS} = 0$ ($C_{DV} = 0$ and $C_{DS} = 4\ \mathrm{GeV}^{-1}$) to generate a stiff (soft) enough dark matter EOS [51]. It should be noted that a too large C_{DS}

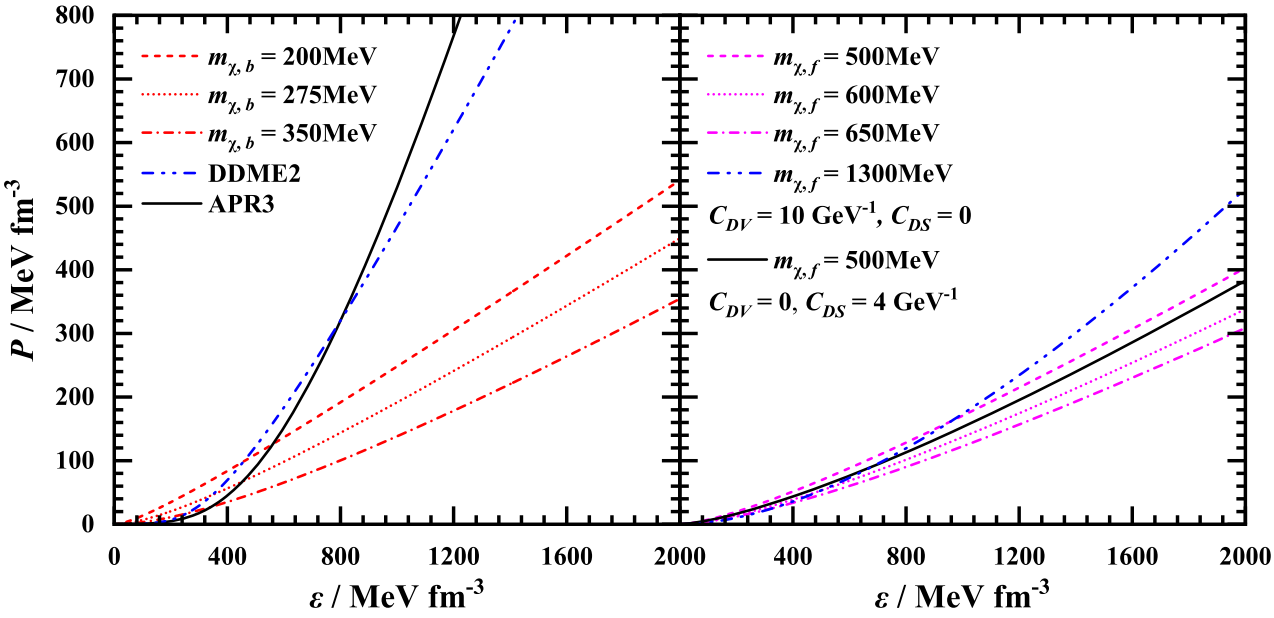

FIG. 1. Dark matter EOSs with different particle masses and interactions and different normal matter EOSs. Left panel: the black solid (blue dash dotted) line is the APR3 (DDME2) EOS represents the normal matter. The red lines with different types are self-interacting bosonic dark matter EOSs with the coupling constant $\lambda = \pi$ and the particle mass $m_{\chi,b} = 200$, 275, and 350 MeV. Right panel: the black solid (blue dash dotted) line is the self-interacting fermionic dark matter EOS with the attractive interaction $C_{DS} = 4$ GeV^{-1} and $C_{DV} = 0$ (the repulsive interaction $C_{DS} = 0$ and $C_{DV} = 10$ GeV^{-1}) and the particle mass $m_{\chi,f} = 500$ MeV ($m_{\chi,f} = 1300$ MeV). The magenta lines with different types are dark matter EOSs described by ideal Fermi gas with the particle mass $m_{\chi,f} = 500$, 600, and 650 MeV.

will induce a nonmonotonic relation between the pressure and the energy density of dark matter EOS.

F. EOS of normal matter

In order to meet the constraints of the GW170817 event and the NICER observational data, we adopt the APR3 EOS (soft) [56] to represent the normal matter EOS. For comparison, we also presented the results obtained using the DDME2 EOS (stiff) [57] as the normal matter EOS, and show the influences of different normal matter EOSs on the macroscopic properties of DANSs. In addition, if the dark matter EOSs is sufficiently stiff, the maximum mass of DANSs constructed with these normal matter EOSs may exceed that of normal neutron stars, and the mass-radius (M-R) relation of DANSs is no longer a curve but extends to a M-R plane [53,58,59].

Finally, the dark matter EOSs with different particle masses and self-interactions, and the different normal matter EOSs used are shown in Fig. 1. It is demonstrated that for dark matter modeled as self-interacting bosons and ideal Fermi gas, the dark matter EoS become softer with the increase of the dark matter particle mass. For self-interacting fermionic dark matter, the repulsive interaction represented by $C_{DV} > 0$ will stiffen the dark matter EOS, while the attractive interaction represented by $C_{DS} > 0$ will soften the dark matter EOS. Moreover, the dark matter particle mass $m_{\chi,f} = 500$ MeV ($m_{\chi,f} = 1300$ MeV) for $C_{DV} = 0$ and $C_{DS} = 4$ GeV^{-1} ($C_{DV} = 10$ GeV^{-1} and $C_{DS} = 0$) is adopted, thus the self-interacting fermionic dark matter EOSs can have a similar stiffness as the ideal Fermi gas EOS with the particle mass $m_{\chi,f} \sim 600$ MeV.

III. RELATIONS OF TIDAL DEFORMABILITY AND NORMAL MATTER RADIUS OF DANS

A. Macroscopic properties of DANSs

Based on the two fluid TOV equations, the relations of the mass and the normal matter radius ($M - R_N$) of DANSs, as well as the mass-tidal deformability ($M - \Lambda$) relations, can be obtained by providing a normal matter EOS and a dark matter EOS. In Fig. 2, the influences of different dark matter mass fractions ($F_X = M_D/M$) on the $M - R_N$ (left panel) and $M - \Lambda$ (right panel) relations of DANSs are shown, where the normal matter EOS is the APR3 EOS and the particle mass of self-interacting bosonic dark matter is $m_{\chi,b} = 275$ MeV. The $M - R_N$ and $M - \Lambda$ relations of normal neutron stars (without the dark matter) are also displayed for comparison. Here we focus on the normal matter radius R_N. The dark matter radius R_D can be hardly detected because the dark matter is electromagnetically dark, but the R_D can have a significant impact on the tidal deformability of DANSs [24,60].

From the left panel of Fig. 2, it is shown that the $M - R_N$ relations of DANSs will extend to a series of curves (dashed

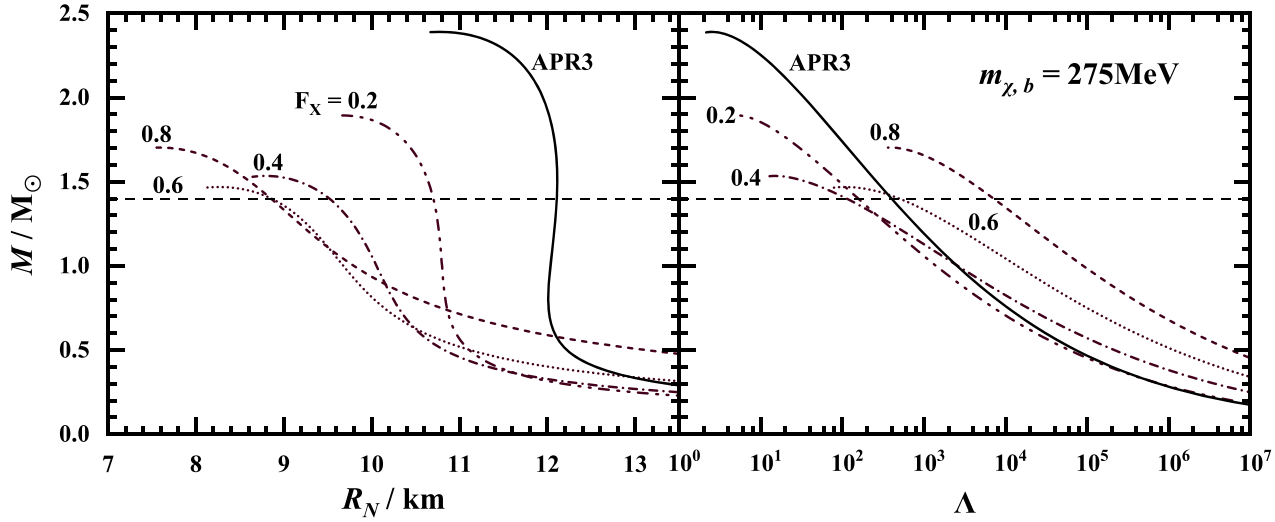

FIG. 2. The influences of different dark matter mass fractions ($F_X = M_D/M$) on the $M - R_N$ (left) and $M - \Lambda$ relations (right) of DANSs (dashed lines), where the normal matter EOS is the APR3 EOS and the particle mass of self-interacting bosonic dark matter is $m_{\chi,b} = 200$ MeV. The $M - R_N$ and $M - \Lambda$ relations of normal neutron stars (solid lines) calculated by the APR3 EOS are also shown.

lines) instead of one curve (solid line) with the change of dark matter mass fraction F_X. If the F_X takes continuous values instead of discrete values, these $M - R_N$ curves will form a $M - R_N$ plane, which means there are multiple DANSs with the same mass but different normal matter radii. This feature of DANSs is similar to that of twin stars [61]. However, in the $M - R_N$ relations containing twin stars, only two different radii are allowed for the normal neutron stars with the same mass [62], thus the twin stars can be distinguished from the DANSs through observations. Due to the wide range of the R_N at a fixed stellar mass of DANSs, induced by the variation of the F_X, the $M - R_N$ relations basically satisfy the constraints of existing observational data, and it is difficult to prove the absence of dark matter in neutron stars only through the existing observations, but the amount of dark matter in the DANSs can be constrained through these observations [39]. Additionally, as the F_X increases, the maximum mass of DANS will decreases firstly and then increases [63,64], and the R_N will decreases [44,58] (but for large F_X, the R_N of low mass DANSs may increase).

Unlike the normal matter radius R_N, the tidal deformability Λ of DANSs in the right panel of Fig. 2 decreases first and then increases with the increase of the dark matter mass fraction F_X. Moreover, when the F_X is high ($\sim$0.8), the Λ of DANSs will become very large [27] (for example, the Λ of DANSs with a mass of $1.4M_\odot$ can reach $\Lambda_{1.4} \sim 8000$) compared to that of normal neutron stars (for the APR3 EOS, $\Lambda_{1.4} \sim 400$). This large Λ of DANSs is caused by the large dark matter radius R_D. For a higher F_X, $R_D > R_N$ (see the lower panel of Fig. 5), so even if the R_N

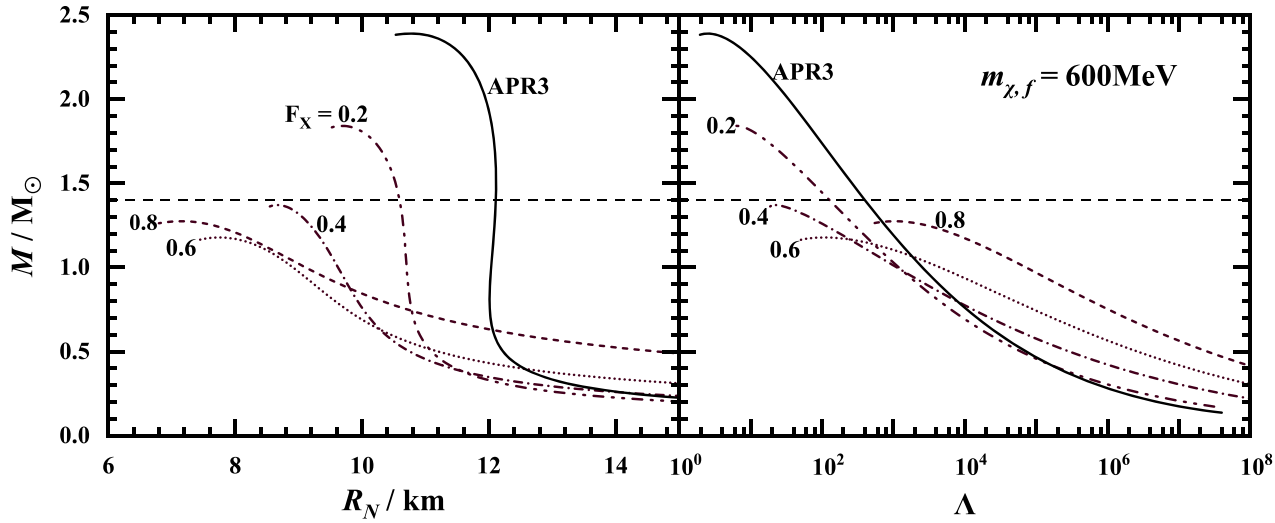

FIG. 3. The same as Fig. 2, but the dark matter is modeled by ideal Fermi gas and the particle mass is $m_{\chi,f} = 600$ MeV.

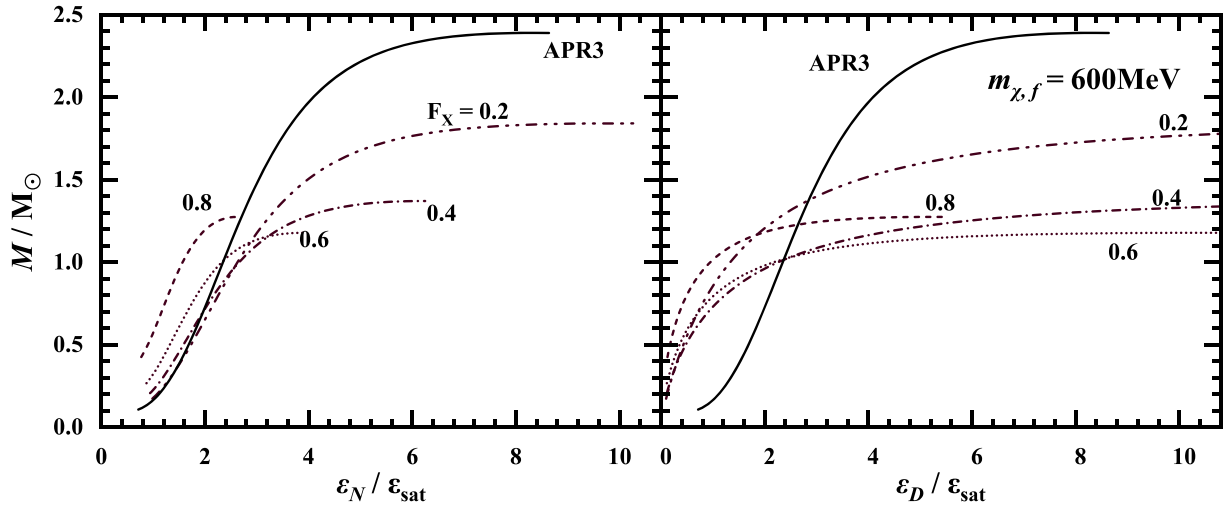

FIG. 4. The left (right) panel is the relation of the mass and the normal (dark) matter central energy density $M - \varepsilon_N$ ($M - \varepsilon_D$) of DANSs. The ε_{sat} is the energy density correspond to the nuclear saturation density. The parameters are the same as those in Fig. 3.

is small (see the left panel of Fig. 2), the total radius R is determined by the larger R_D, and it will result in a large Λ of a DANS [see Eq. (8)] greater than the Λ of a normal neutron star.

For the dark matter modeled as the ideal Fermi gas, the influence of the dark matter mass fraction F_X on the normal matter radius R_N and the tidal deformability Λ of DANSs are shown in Fig. 3. Similar to Fig. 2, the $M - R_N$ and $M - \Lambda$ relations of DANSs have also extended to a series of curves. However, compared to the self-interacting bosonic dark matter, a larger particle mass is need in the ideal Fermi gas EOS to support DANSs with similar mass. This is due to the lack of self-interaction in the ideal Fermi gas. If the attractive interaction ($C_{DS} > 0$) is considered in the fermionic dark matter EOSs, only a smaller particle mass is needed for the dark matter EOSs to support DANSs with similar mass. Contrarily, if the repulsive interaction ($C_{DV} > 0$) is considered in the fermionic dark matter EOSs, a larger particle mass is needed for the dark matter EOSs to support DANSs with similar mass. The influence of the self-interaction on DANSs with fermionic dark matter EOSs will be discussed in detail later.

It is previously found that the mass of DANSs should decrease as the dark matter central energy density ε_D increases [51]. However, it should be noted that a larger dark matter mass fraction F_X does not necessarily correspond to a larger ε_D, because there may be a smaller normal matter central energy density ε_N. In Fig. 4, we demonstrate the effect of increasing F_X on the $M - \varepsilon_N$ ($M - \varepsilon_D$) relations of DANSs in the left (right) panel. The results show that as the F_X increases, the ε_D should increase first and then decrease. The decrease of the ε_D at a large F_X (the ε_N also decrease so the large F_X can be maintained) induce the increase of the mass of DANSs. Moreover, it is shown in Figs. 2 and 3 that there is an increase of R_N for DANSs with a large F_X. This is related to the decrease of the ε_N of DANSs (see the $M - \varepsilon_N$ relation of $F_X = 0.8$ in Fig. 4). Note that the decrease of ε_D, which is not as obvious as the decrease of ε_N, ensures the large value of F_X.

Compared to DANSs ($F_X < 0.5$) with the mirror dark matter model [43,65], a larger dark matter mass fraction ($F_X < 0.8$) is utilized in our work. The reason is that for DANSs with the mirror dark matter model, if the normal matter radius is replaced by the dark matter radius, the mass-radius relations of $F_X > 0.5$ are exactly the same as the mass-radius relations of $F_X < 0.5$. For example, the mass of DANSs with $F_X = 0.75$ is the same as that of DANSs with $F_X = 0.25$, and the dark matter radius of DANSs with $F_X = 0.75$ is also the same as the normal matter radius of DANSs with $F_X = 0.25$. However, for other dark matter models, this situation is not valid, so it is necessary to investigate DANSs with larger dark matter mass fractions.

Additionally, for DANSs with a relatively small dark matter mass fraction ($F_X < 0.5$), the stars can acquire enough dark matter through accretion during its billion-year long lifetime [65]. However, a higher dark matter density may exist at the center of the galaxies or in the early Universe [4,58], so neutron stars may form DANSs with a larger dark matter mass fraction ($F_X \sim 0.8$ [58]) through the accretion in such environment. Furthermore, the merger of a normal neutron star and a pure dark matter star (with mass above $1M_\odot$) can also lead to the formation of DANSs with a large F_X [4,53,63,64], and the formation of such DANSs could be relatively easy to discover due to the high energy phenomenon [66].

B. Negative correlation between tidal deformability and normal matter radius

To illustrate the effect of dark matter on the normal matter radius R_N and the (dimensionless) tidal deformability Λ of DANSs intuitively, the upper panel of Fig. 5

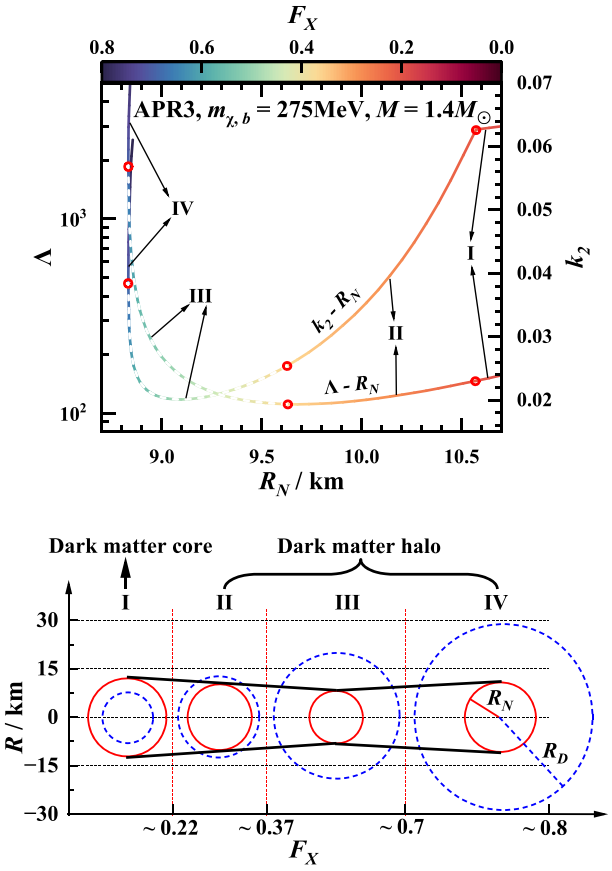

FIG. 5. Upper panel: the $k_2 - R_N$ and $\Lambda - R_N$ relations of DANSs with a fixed stellar mass ($1.4M_\odot$) at different dark matter mass fractions F_X. The dashed lines labeled with III represent the range of F_X corresponding to the negative correlation between the tidal deformability Λ and the normal matter radius R_N, while the solid lines (I, II, and IV) represent the positive correlation between the Λ and the R_N. Lower panel: the relative size of the R_N (red solid circle) and the R_D (blue dashed circle) of DANSs ($1.4M_\odot$) at different F_X values (I, II, III, and VI). The normal matter EOS and the dark matter parameters adopt the same as those used in Fig. 2.

shows the relation of R_N and Λ of DANSs with a fixed stellar mass ($1.4M_\odot$) at different dark matter mass fractions F_X. Here we only show the result of self-interacting bosonic dark matter, and the result of fermionic dark matter (with or without self-interaction) is similar to that. From the upper panel of Fig. 5, it can be seen that with the increase of F_X, both the R_N and the Λ initially decrease and then increase. However, their decreases or increases are not simultaneous. That is to say, in a specific range of F_X (indicated by the dashed line labeled III in the upper panel of Fig. 5), the Λ increases while the R_N decreases. As a comparison, this phenomenon does not exist in twin stars. Although the mass of twin stars are the same, the one with a smaller radius must have a smaller tidal deformability [61]. Therefore, the negative correlation between the tidal deformability Λ and the normal matter radius R_N of the DANSs at a fixed stellar mass may served as a clue to prove the presence of dark matter in neutron stars.

To further investigate the negative correlation between the tidal deformability Λ and the normal matter radius R_N of DANSs, the $k_2 - R_N$ relation of DANSs with a mass of $1.4M_\odot$ at different F_X is also shown in the upper panel of Fig. 5 (where k_2 is the tidal Love number), and the relative size of the R_N and the R_D of those DANSs is presented in the lower panel of Fig. 5. For DANSs with a relatively small F_X (labeled with I and II in Fig. 5), an increase of F_X leads to a decrease of R_N, k_2 and Λ. Although in the stage II (beginning with the kink of the $k_2 - R_N$ curve) the total radius $R = R_D > R_N$ (i.e., dark matter halo) increases with the increase of F_X, the decreasing k_2 dominates the decrease of tidal deformability Λ [see Eq. (8)]. Conversely, the increase of $R = R_D$ will dominate as the F_X further increases (III in Fig. 5), so the Λ will increase while the R_N remains decreasing. This range of F_X corresponds to the negative correlation between the tidal deformability Λ and the normal matter radius R_N. When the dark matter accounts for a significant portion in DANSs (VI in Fig. 5), the Λ and the R_N show a positive correlation again. It should be noted that for the DANSs with different masses, the specific range of F_X corresponding to the negative correlation between the tidal deformability Λ and the normal matter radius R_N varies (see Fig. 6).

C. Influences of dark matter parameters and normal matter EOSs

The normal matter radius R_N and the tidal deformablity Λ of DANSs are also influenced by the parameters (the particle mass and the self-interaction) of the dark matter EOSs and the normal matter EOSs. In order to investigate the generality of the negative correlation between the Λ and the R_N, in Fig. 6, the three panels, (a), (b), and (c), show the effect of the particle mass $m_{\chi,b}$ of self-interacting bosonic dark matter on the Λ and R_N, and the panels (b) and (d) show the effect of the normal matter EOSs. The discontinuous solid lines [such as the $2M_\odot$ DANSs in the panel (a)] indicate that for some ranges of F_X, the given EOSs of normal matter and dark matter cannot support the DANSs with a relatively high mass ($2M_\odot$).

The three panels (a), (b), and (c) of Fig. 6 show that an increase of $m_{\chi,b}$ will induce a decrease of tidal deformability Λ and normal matter radius R_N of the DANSs with a large F_X. For a larger $m_{\chi,b}$, the self-interacting bosonic dark matter tends to accumulate within the DANSs to form a dark matter core rather than a dark matter halo, and the heavier core has a stronger gravitational effect on the normal matter, resulting in a decrease of R_N. Similarly, the larger $m_{\chi,b}$ also lead to a smaller total radius R of DANSs, which induces a smaller Λ. Furthermore, the increase of $m_{\chi,b}$ will induce the negative correlation between the tidal deformability Λ and the normal matter radius R_N (dashed lines) to occur at a lower DANS mass. For $m_{\chi,b} = 200$ MeV, this negative

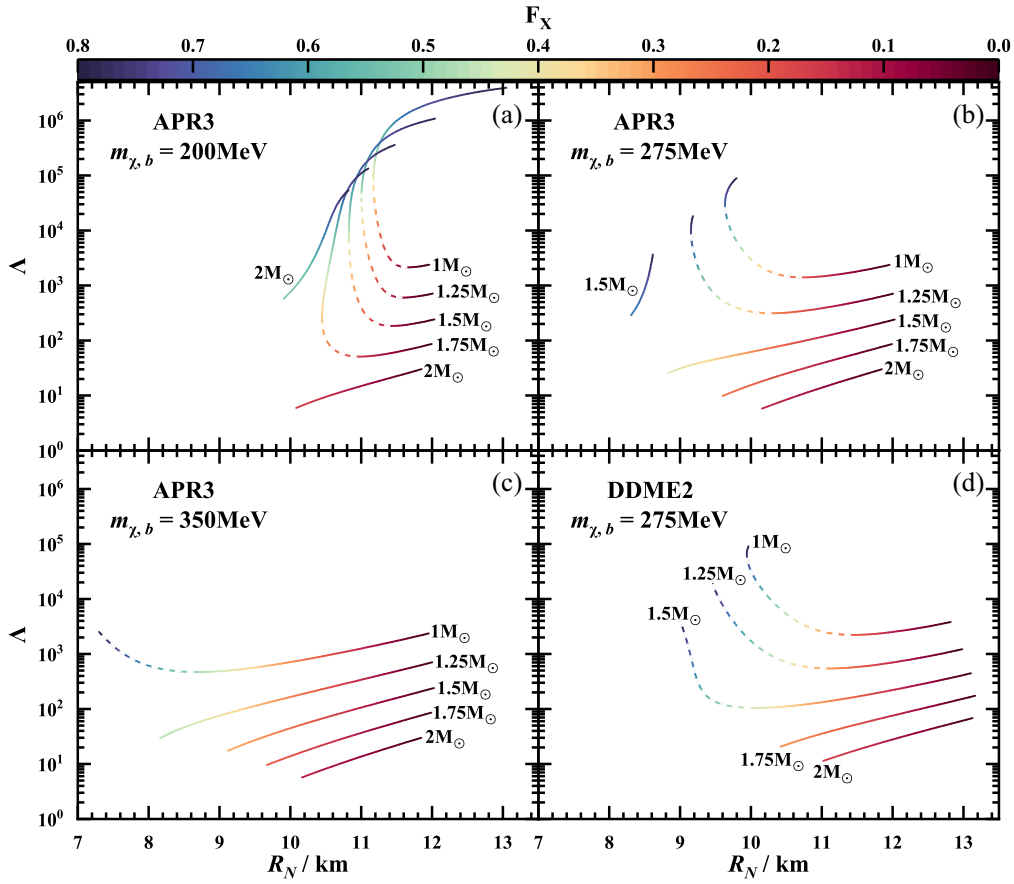

FIG. 6. The effects of the particle mass $m_{\chi,b}$ of self-interacting dark matter and the normal matter EOSs on the relations of normal matter radius R_N and tidal deformability Λ of DANSs (with masses of 1, 1.25, 1.5, 1.75, and $2M_\odot$) at different dark matter mass fractions F_X. In panels (a), (b), and (c), the $m_{\chi,b}$ adopts 200, 275, and 350 MeV, and the normal matter is described by the APR3 EOS. In panel (d), the $m_{\chi,b}$ adopts 275 MeV, and the normal matter is described by the DDME2 EOS. The dashed and solid lines are similar to those in Fig. 5.

correlation of DANSs with a mass of $1.75M_\odot$ is displayed in the panel (a) of Fig. 6, but for $m_{\chi,b} = 275$ MeV, that of DANSs only occurs when the mass of DANSs is smaller than $1.5M_\odot$ (panel (b) of Fig. 6). If the $m_{\chi,b}$ further increases ($m_{\chi,b} > 350$ MeV), then only the DANSs with a mass around $1M_\odot$ or less than that are likely to show the negative correlation between the tidal deformability Λ and the normal matter radius R_N. Conversely, a smaller particle mass ($m_{\chi,b} < 200$ MeV) will lead to a less obvious decrease in the R_N of DANSs with this negative correlation during the increase of Λ, making it difficult to distinguish such DNASs through the normal matter radius R_N. Therefore, we only investigate the macroscopic properties of DANSs when the $m_{\chi,b}$ is at around 300 MeV. Additionally, a stiffer normal matter EOS (panel (d) of Fig. 6) can cause this negative correlation to occur when the DANSs have a larger mass ($1.5M_\odot$), but the effect of normal matter EOSs is not as significant as the effect of varying $m_{\chi,b}$. Overall, for the self-interacting bosonic dark matter, the negative correlation between the tidal deformability and the normal matter radius of DANSs is universal when changing the particle mass of dark matter and the normal matter EOS. Furthermore, it is important to emphasize that the effective parameter in Eq. (10) is $m_{\chi,b}^4/\lambda$, so the effect of decreasing λ is the same as the effect of increasing $m_{\chi,b}$. If the λ is changed, the tidal deformability and the normal matter radius of DANSs at a fixed $m_{\chi,b}$ will also change.

Similarly, the effects of varying the particle mass $m_{\chi,f}$ of dark matter modeled as ideal Fermi gas and the normal matter EOS on the tidal deformability Λ and the normal matter radius R_N of DANSs is illustrated in Fig. 7. For the dark matter modeled as ideal Fermi gas, a larger particle mass is needed to support DANSs with similar stellar mass compared with the situation in the case of self-interacting bosoninc dark matter. If the bosonic dark matter EOS with the coupling constant $\lambda > \pi$ [32,40] or the attractive self-interacting fermionic dark matter EOS [38,51] is considered, the difference between the particle mass of the fermionic and bosonic dark matter EOSs that can support DANSs with similar mass could disappear. The negative

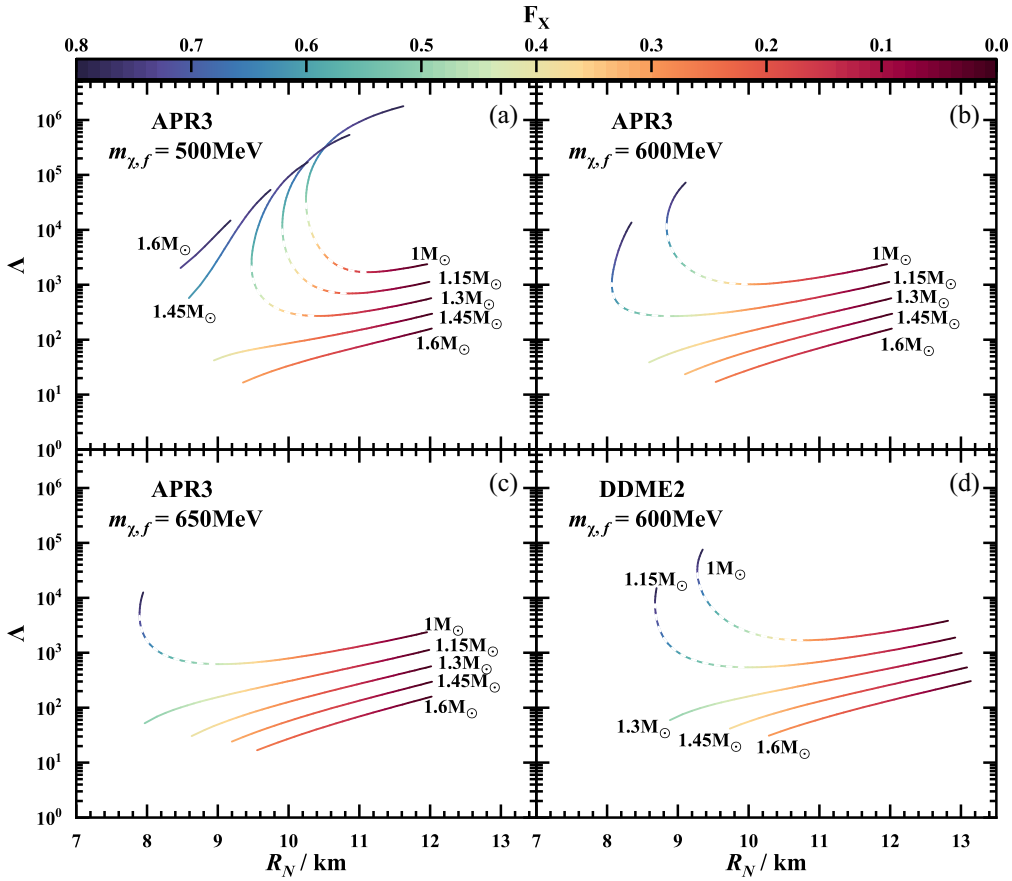

FIG. 7. The same as Fig. 6, but the dark matter is modeled by the ideal Fermi gas, and the particle mass $m_{\chi,f}$ of fermionic dark matter adopts 500, 600, and 650 MeV. The masses of DANSs are 1, 1.15, 1.3, 1.45, and $1.6M_\odot$.

correlation between the tidal deformability Λ and the normal matter radius R_N of DANSs is also presented for the fermionic dark matter, as shown in Fig. 7. The increase of $m_{\chi,f}$ also causes this negative correlation to occur at a lower DANS mass, whereas the effect of modifying the normal matter EOS on this negative correlation is not obvious. As a result, regardless of the types of dark matter (self-interacting bosons or ideal Fermi gas), if there are a series of neutron stars with the same or extremely similar mass in future observation, and the ones with smaller radii have larger tidal deformabilities, it is very likely to imply the existence of dark matter in the neutron stars. Moreover, if the stellar mass of this series of neutron stars is greater than a certain value (for example, $M > 1.25M_\odot$), then it is also possible to constrain the parameters of dark matter (for the self-interacting bosonic dark matter, $m_{\chi,b} < 350$ MeV when $\lambda = \pi$, and for the dark matter modeled as ideal Fermi gas, the $m_{\chi,f}$ is constrained to $m_{\chi,f} < 600$ MeV).

The effect of the self-interaction of fermionic dark matter on the negative correlation between the tidal deformability and the normal matter radius of DANSs is also investigated preliminarily. In Fig. 8, the left (right) panel shows the result of the fermionic dark matter EOS with the particle mass $m_{\chi,f} = 500$ MeV and the interaction parameter $C_{DV} = 0$ and $C_{DS} = 4$ GeV^{-1} ($m_{\chi,f} = 1300$ MeV, $C_{DV} = 10$ GeV^{-1} and $C_{DS} = 0$). In the left panel, due to the softening of the dark matter EOS induced by the attractive interaction ($C_{DS} = 4$ GeV^{-1}), and the stiffening of the dark matter EOS induced by a smaller particle mass ($m_{\chi,f} = 500$ MeV), the fermionic dark matter EOS with the attractive interaction has a similar stiffness of the ideal Fermi gas EOS of $m_{\chi,f} = 600$ MeV (also can be seen in Fig. 1), so these two dark matter EOSs can support DANSs with similar mass ($M = 1.15M_\odot$) when the F_X change from 0 to 0.8 (panel (b) in Fig. 7 and panel (a) in Fig. 8). Conversely, a larger particle mass ($m_{\chi,f} = 1300$ MeV) is needed for the repulsive self-interacting ($C_{DV} = 10$ GeV^{-1} and $C_{DS} = 0$) fermionic dark matter EOS to support DANSs with the mass of $M = 1.15M_\odot$ (panel (b) in Fig. 8). Moreover, for self-interacting fermionic dark matter EOSs with the similar stiffness, a large C_{DV} leads to a significant increase of $m_{\chi,f}$, while a small C_{DS} only slightly reduces the $m_{\chi,f}$.

Although the fermionic dark matter EOSs with repulsive and attractive interactions have the similar stiffness, for a large value of F_X, there are larger values of the normal matter radius R_N and the tidal deformability Λ for DANSs with attractive self-interacting fermionic dark matter

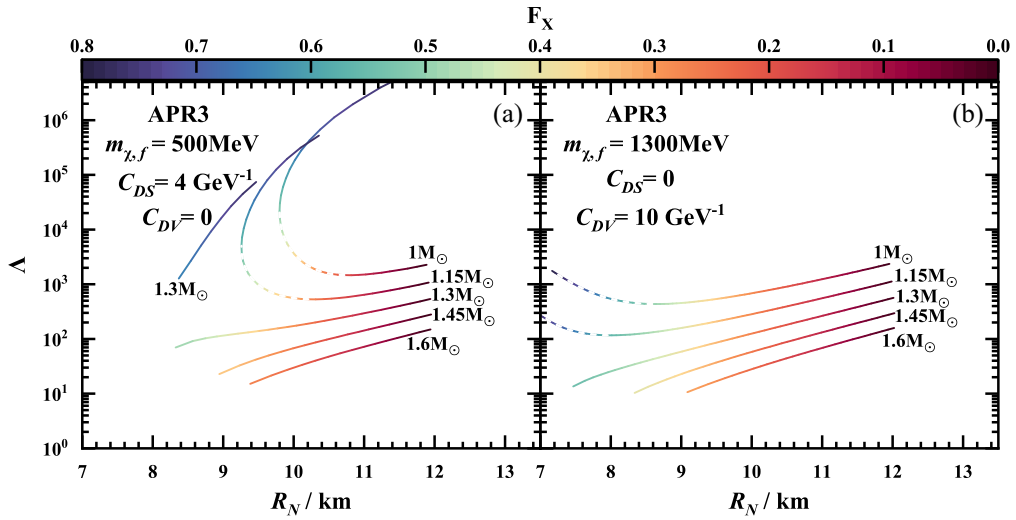

FIG. 8. The same as Fig. 7, but the dark matter is modeled by attractive (panel (a), $C_{DV} = 0$ and $C_{DS} = 4$ GeV^{-1}) or repulsive (panel (b), $C_{DV} = 10$ GeV^{-1} and $C_{DS} = 0$) self-interacting fermions, and the particle mass $m_{\chi,f}$ of fermionic dark matter adopts 500 or 1300 MeV.

(see panel (a) in Fig. 8). Because the Λ of low mass DANSs ($M \sim 1.15M_\odot$) is mainly affected by the low-density range of dark matter EOSs when the F_X is large, and the fermionic dark matter EOS with attractive interaction is stiffer in the low-density region (see the black solid line in the right panel of Fig. 1), which leads to a larger Λ. The large value of R_N for a large F_X is due to the rapid decrease of normal matter central energy density in DANSs with attractive self-interacting fermionic dark matter.

Overall, the negative correlation between the tidal deformability and the normal matter radius of DANSs still exists when considering the self-interacting fermionic dark matter, and the mass of DANSs corresponding to this negative correlation can constrain the parameters of self-interacting fermionic dark matter EOSs. Specifically, if a series of DANSs with this negative correlation and $M > 1.25M_\odot$ are found in future observations, the existence of the attractive self-interaction ($C_{DV} = 0$ and $C_{DS} = 4$ GeV^{-1}) in fermionic dark matter will constrain the $m_{\chi,f}$ to a small value ($m_{\chi,f} < 500$ MeV), while the existence of the repulsive self-interaction ($C_{DV} = 10$ GeV^{-1} and $C_{DS} = 0$) in fermionic dark matter will widen the range of the $m_{\chi,f}$ ($m_{\chi,f} < 1300$ MeV) compared to the situation of dark matter modeled as ideal Fermi gas ($m_{\chi,f} < 600$ MeV). If the self-interaction between the fermions is changed (i.e., the change of C_{DS} and C_{DV}), the constraint on the $m_{\chi,f}$ will change correspondingly.

IV. SUMMARY

It is shown that there is a series of DANSs with the same mass but different dark matter mass fractions, and the ones with smaller normal matter radii have larger tidal deformabilities, i.e., the negative correlation between the tidal deformability and the normal matter radius. This negative correlation does not exist in other types of neutron stars (such as twin stars [61], quark stars [67]). If observations confirm that there is a series of neutron stars with the same or very similar mass, and the ones with smaller radii have greater tidal deformabilities, it may indicate the existence of dark matter in the neutron stars. The interaction among the dark matter particles may be more complex in reality [27,60], the negative correlation between the tidal deformability and the normal matter radius of DANSs is believed to exist even when the dark matter model is changed. In addition, the negative correlation between the tidal deformability and the normal matter radius of DANSs also provides a way to constrain the dark matter parameters.

ACKNOWLEDGMENTS

We would like to thank S. N. Wei for useful suggestions about the self-interacting fermionic dark matter model. This work is supported by NSFC (Grants No. 12375144, No. 11975101) and Guangdong Natural Science Foundation (Grants No. 2022A1515011552 and No. 2020A151501820).

[1] G. Bertone and T. M. P. Tait, Nature (London) **562**, 51 (2018).
[2] G. Bertone and D. Hooper, Rev. Mod. Phys. **90**, 045002 (2018).
[3] J. Ellis, G. Hütsi, K. Kannike, L. Marzola, M. Raidal, and V. Vaskonen, Phys. Rev. D **97**, 123007 (2018).
[4] F. Sandin and P. Ciarcelluti, Astropart. Phys. 09 (**2009**) 278.
[5] T. E. Riley *et al.*, Astrophys. J. Lett. **918**, L27 (2021).
[6] M. C. Miller *et al.*, Astrophys. J. Lett. **918**, L28 (2021).
[7] T. E. Riley *et al.*, Astrophys. J. Lett. **887**, L21 (2019).
[8] M. C. Miller *et al.*, Astrophys. J. Lett. **887**, L24 (2019).
[9] Z. Miao, A. Li, and Z. G. Dai, Mon. Not. R. Astron. Soc. **515**, 5071 (2022).
[10] J. J. Li, A. Sedrakian, and M. Alford, Phys. Rev. D **104**, L121302 (2021).
[11] B. P. Abbott *et al.*, Phys. Rev. Lett. **119**, 161101 (2017).
[12] B. P. Abbott *et al.*, Phys. Rev. Lett. **121**, 161101 (2018).
[13] N. Jiang and K. Yagi, Phys. Rev. D **101**, 124006 (2020).
[14] J. L. Jiang, S.-P. Tang, Y.-Z. Wang, Y.-Z. Fan, and D.-M. Wei, Astrophys. J. **892**, 55 (2020).
[15] S. Yang, D. Wen, J. Wang, and J. Zhang, Phys. Rev. D **105**, 063023 (2022).
[16] H. O. Silva, A. Miguel Holgado, A. Cárdenas-Avendaño, and N. Yunes, Phys. Rev. Lett. **126**, 181101 (2021).
[17] N. Zhang, D. H. Wen, and H. Y. Chen, Phys. Rev. C **99**, 035803 (2019).
[18] H. Y. Sun and D. H. Wen, Phys. Rev. C **108**, 025801 (2023).
[19] A. Kanakis-Pegios, P. S. Koliogiannis, and C. C. Moustakidis, Symmetry **13**, 183 (2021).
[20] Y. X. Li, H. Chen, D. Wen, and J. Zhang, Eur. Phys. J. A **57**, 31 (2021).
[21] J. Zhang, D. H. Wen, and Y. X. Li, Commun. Theor. Phys. **73**, 115302 (2021).
[22] N. K. Patra, A. Venneti, S. M. Adil Imam, A. Mukherjee, and B. K. Agrawal, Phys. Rev. C **107**, 055804 (2023).
[23] M. Deliyergiyev, A. Del Popolo, L. Tolos, M. Le Delliou, X. Lee, and F. Burgio, Phys. Rev. D **99**, 063015 (2019).
[24] A. E. Nelson, S. Reddy, and D. Zhou, J. Cosmol. Astropart. Phys. 07 (2019) 012.
[25] Z. Rezaei, Mon. Not. R. Astron. Soc. **524**, 2015 (2023).
[26] H. M. Liu, J.-B. Wei, Z.-H. Li, G. F. Burgio, and H.-J. Schulze, Phys. Dark Universe **42**, 101338 (2023).
[27] B. K. K. Lee, M. Chu, and L. M. Lin, Astrophys. J. **922**, 242 (2021).
[28] J. Ellis, A. Hektor, G. Hütsi, K. Kannike, L. Marzola, M. Raidal, and V. Vaskonen, Phys. Lett. B **781**, 607 (2018).
[29] H. R. Rüter, V. Sagun, W. Tichy, and T. Dietrich, Phys. Rev. D **108**, 124080 (2023).
[30] M. Bezares and D. Viganò, and C. Palenzuela, Phys. Rev. D **100**, 044049 (2019).
[31] C. J. Horowitz and S. Reddy, Phys. Rev. Lett. **122**, 071102 (2019).
[32] D. R. Karkevandi, S. Shakeri, V. Sagun, and O. Ivanytskyi, Phys. Rev. D **105**, 023001 (2022).
[33] S. Bhattacharya, B. Dasgupta, R. Laha, and A. Ray, Phys. Rev. Lett. **131**, 091401 (2023).
[34] S. Banerjee, S. Bera, and D. F. Mota, J. Cosmol. Astropart. Phys. 03 (2023) 041.
[35] I. Goldman, R. N. Mohapatra, S. Nussinov, D. Rosenbaum, and V. Teplitz, Phys. Lett. B **725**, 200 (2013).
[36] H. C. Das, A. Kumar, B. Kumar, S. K. Biswal, T. Nakatsukasa, A. Li, and S K Patra, Mon. Not. R. Astron. Soc. **495**, 4893 (2020).
[37] P. Thakur, T. Malik, A. Das, T. K. Jha, and C. Providência, Phys. Rev. D **109**, 043030 (2024).
[38] Z. Miao, Y. Zhu, A. Li, and F. Huang, Astrophys. J. **936**, 69 (2022).
[39] O. Ivanytskyi and V. Sagun, Phys. Rev. D **102**, 063028 (2020).
[40] S. Shakeri and D. R. Karkevandi, Phys. Rev. D **109**, 043029 (2024).
[41] E. Giangrandi, V. Sagun, O. Ivanytskyi, C. Providência, and T. Dietrich, Astrophys. J. **953**, 115 (2023).
[42] S. C. Leung, M. C. Chu, and L. M. Lin, Phys. Rev. D **85**, 471 (2012).
[43] F. Sandin and P. Ciarcelluti, Phys. Lett. B **695**, 19 (2011).
[44] K. L. Leung, M. Chu, and L. M. Lin, Phys. Rev. D **105**, 123010 (2022).
[45] N. Rutherford, G. Raaijmakers, C. Prescod-Weinstein, and A. Watts, Phys. Rev. D **107**, 103051 (2023).
[46] A. Maselli, P. Pnigouras, N. G. Nielsen, C. Kouvaris, and K. D. Kokkotas, Phys. Rev. D **96**, 023005 (2017).
[47] M. I. Gresham and K. M. Zurek, Phys. Rev. D **99**, 083008 (2019).
[48] M. Colpi, S. L. Shapiro, and I. Wasserman, Phys. Rev. Lett. **57**, 2485 (1986).
[49] J. R. Oppenheimer and G. M. Volkoff, Phys. Rev. **55**, 374 (1939).
[50] S. N. Wei and Z. Q. Feng, Chin. Phys. C **46**, 043101 (2022).
[51] Q. F. Xiang, L. Clark, A. Béché, and J. Verbeeck, Phys. Rev. D **89**, 025803 (2014).
[52] V. Desjacques, A. Kehagias, and A. Riotto, Phys. Rev. D **97**, 023529 (2018).
[53] M. Hippert, E. Dillingham, H. Tan, D. Curtin, J. Noronha-Hostler, and N. Yunes, Phys. Rev. D **107**, 115028 (2023).
[54] T. Hinderer, B. D. Lackey, R. N. Lang, and J. S. Read, Phys. Rev. D **81**, 123016 (2010).
[55] A. Kanakis-Pegios, P. S. Koliogiannis, and C. C. Moustakidis, Phys. Rev. C **102**, 055801 (2020).
[56] A. Akmal and V. R. Pandharipande, Phys. Rev. C **156**, 2261 (1997).
[57] G. A. Lalazissis, T. Nikšić, D. Vretenar, and P. Ring, Phys. Rev. C **71**, 024312 (2005).
[58] X. Y. Li, F. Y. Wang, and K. S. Cheng, J. Cosmol. Astropart. Phys. 10 (2012) 031.
[59] R. Zöllner, M. Ding, and B. Kämpfer, Particles **6**, 217 (2023).
[60] P. Routaray, S. R. Mohanty, H. C. Das, S. Ghosh, P. J. Kalita, V. Parmar, and B. Kumar, J. Cosmol. Astropart. Phys. 10 (2023) 073.
[61] D. Blaschke *et al.*, Astrophysical aspects of general relativistic mass twin stars, in *Topics on Strong Gravity*, edited by C. A. Zen Vasconcellos (World Scientific, Singapore, 2020), pp. 207–256.

[62] M. G. Alford and S. Han, Eur. Phys. J. A **52**, 62 (2016).
[63] R. F. Diedrichs, N. Becker, C. Jockel, J.-E. Christian, L. Sagunski, and J. Schaffner-Bielich, Phys. Rev. D **108**, 064009 (2023).
[64] C. Jockel and L. Sagunski, Particles **7**, 52 (2024).
[65] R. Ciancarella, F. Pannarale, A. Addazi, and A. Marcianò, Phys. Dark Universe **32**, 100796 (2021).
[66] K. Barbary *et al.*, Astrophys. J. **690**, 1358 (2008).
[67] M. B. Albino, R. Fariello, and F. S. Navarra, Phys. Rev. D **104**, 083011 (2021).